

---

# NE<sub>X</sub>ON-BAYES: A BAYESIAN APPROACH TO NETWORK ESTIMATION INFORMED BY ORDINAL COVARIATES

---

**Joseph Feast**  
MRC Biostatistics Unit  
University of Cambridge  
Cambridge, CB2 0SR, UK  
joseph.feest@mrc-bsu.cam.ac.uk

**Hélène Ruffieux**  
MRC Biostatistics Unit  
University of Cambridge  
Cambridge, CB2 0SR, UK  
helene.ruffieux@mrc-bsu.cam.ac.uk

**Camilla Lingjærde**  
Department of Mathematics  
University of Oslo  
Oslo, N-0316, Norway  
camiling@math.uio.no

**Xiaoyue Xi**  
MRC Biostatistics Unit  
University of Cambridge  
Cambridge, CB2 0SR, UK  
xiaoyue.xi@mrc-bsu.cam.ac.uk

September 1, 2025

## ABSTRACT

**Motivation:** In heterogeneous disease settings, accounting for intrinsic sample variability is crucial for obtaining reliable and interpretable omic network estimates. However, most graphical model analyses of biomedical data assume homogeneous conditional dependence structures, potentially leading to misleading conclusions. To address this, we propose a joint Gaussian graphical model that leverages sample-level ordinal covariates (e.g., disease stage) to account for heterogeneity and improve the estimation of partial correlation structures.

**Results:** Our modelling framework, called NExON-Bayes, extends the graphical spike-and-slab framework to account for ordinal covariates, jointly estimating their relevance to the graph structure and leveraging them to improve the accuracy of network estimation. To scale to high-dimensional omic settings, we develop an efficient variational inference algorithm tailored to our model. Through simulations, we demonstrate that our method outperforms the vanilla graphical spike-and-slab (with no covariate information), as well as other state-of-the-art network approaches which exploit covariate information. Applying our method to reverse phase protein array data from patients diagnosed with stage I, II or III breast carcinoma, we estimate the behaviour of proteomic networks as breast carcinoma progresses. Our model provides insights not only through inspection of the estimated proteomic networks, but also of the estimated ordinal covariate dependencies of key groups of proteins within those networks, offering a comprehensive understanding of how biological pathways shift across disease stages.

**Availability and Implementation:** A user-friendly R package for NExON-Bayes with tutorials is available on Github at [github.com/jf687/NExON](https://github.com/jf687/NExON).

**Keywords** Gaussian Graphical Model, Ordinal Data, Patient Heterogeneity, Scalable Variational Inference.

## 1 Introduction

Graphical models are useful tools to uncover complex dependence structures between molecular variables and shed light on the biological mechanisms underlying disease. In Gaussian graphical models (GGMs), typically employed for the analysis of omic data, the partial correlations between nodes can be derived from the off-diagonal elements of the inverse covariance (precision) matrix. Various approaches for GGM estimation have been developed using frequentist and Bayesian approaches. Frequentist approaches are based on penalised maximum likelihood estimation and include neighbourhood selection [Meinshausen and Bühlmann, 2006], the graphical lasso [Friedman et al., 2008] and the graphical SCAD [Fan et al., 2009]. Bayesian methods place a shrinkage prior on the precision matrix entries and include the Bayesian graphical lasso [Wang, 2012], the graphical horseshoe [Li et al., 2019] and the graphical

spike-and-slab [Wang, 2015]. These methods all assume homogeneous dependence structures across all samples, an assumption that is often unrealistic in practical settings where, for example, samples might be collected from patients across different conditions, such as different disease severities or treatment regimes.

More recently, methods have been developed to jointly estimate graphical models across multiple networks, reflecting such conditions. Joint methods estimate network structures through sharing information between networks when appropriate, while ideally retaining network-specific differences. Several approaches for joint estimation of multiple GGMs have been proposed. Frequentist approaches extend the penalised likelihood framework to add penalty parameters that encourage similarity between network-specific precision matrices [Guo et al., 2011, Ma and Michailidis, 2016, Lingjærde and Richardson, 2023], whilst Bayesian approaches use priors to encourage the potential sharing of network structures [Li et al., 2019, Lingjærde et al., 2024]. Such methods have been used, for example, to estimate the proteomic networks of breast cancer patients with different subtype diagnoses, where the expected similarities between networks are leveraged in the joint estimation [Lingjærde and Richardson, 2023].

Existing joint estimation approaches often treat networks as exchangeable, which in some cases can inhibit statistical power. For example, when the covariates used to define subgroups have a natural ordering, the assumption of exchangeability both omits useful information that could be leveraged in the estimation and limits the potential insight into how those covariates affect graphical structure. A related set of more recent approaches build on this idea by making GGMs dependent on covariates. Despite working for a wide range of covariates, these approaches do not ensure the positive definiteness of the precision matrix and often lack scalability, which seems to hamper widespread adoption [Helwig et al., 2024, Chen et al., 2024].

Here we present NExON-Bayes, a Bayesian approach to network estimation informed by ordinal covariates. NExON-Bayes builds on the standard graphical spike-and-slab model of Wang et al. (2015) Wang [2015], and introduces a sub-model that characterises the dependence between edge inclusion probabilities and sample-level ordinal covariate data, rather than modelling the entries of the precision matrix, as done in other covariate-dependent approaches. This modelling framework allows us to develop a deterministic inference algorithm that is more scalable than existing alternatives in the literature.

This paper is organised as follows. Section 2 introduces the terminology and notation used throughout the article, our proposed model, and the variational inference algorithm. Next, Section 3 assesses the performance of our approach by benchmarking the model against several competitors through simulations, and investigates its benefits in a real-life setting where we estimate the proteomic networks of breast carcinoma patients. Finally, Section 4 summarises our contributions and avenues for extensions of this work.

## 2 Methods

### 2.1 Terminology and notation

A graphical model is a probabilistic framework that represents dependencies among a set of random variables. It is represented by  $\mathcal{G} = (\mathcal{V}, E)$ , where  $\mathcal{V} = \{1, \dots, P\}$  is the set of nodes (variables) and  $E$  is the set of undirected edges between them. In a Gaussian graphical model (GGM) the nodes represent random variables from a multivariate Gaussian distribution, whilst the edges represent conditional dependence between the variables that they connect. A GGM assumes that  $N$  samples of  $P$  variables are independently and identically distributed (i.i.d.) according to

$$\mathbf{y}_n \sim \mathcal{N}_P(\mathbf{0}, \mathbf{\Omega}^{-1}), \quad n = 1, \dots, N,$$

where  $\mathbf{\Omega}$  is the positive definite inverse covariance matrix, known as the *precision matrix*. In this work, we consider the case in which each of the  $N$  samples is characterised by a sample-level ordinal covariate  $a$  taking values in a set  $\mathcal{A}$ . We further assume sample homogeneity within groups defined by the same covariate value, rather than across all samples. Specifically,

$$\mathbf{y}_n^{(a)} \sim \mathcal{N}_P(\mathbf{0}, (\mathbf{\Omega}^{(a)})^{-1}), \quad n = 1, \dots, N_a, \tag{1}$$

where  $\mathbf{\Omega}^{(a)}$  is the precision matrix specific to group  $a \in \mathcal{A}$ ,<sup>1</sup> and  $N_a$  is the number of samples within the dataset specific to a covariate value  $a$ . A covariate-specific dataset can then be denoted as  $\mathbf{Y}^{(a)} = (\mathbf{y}_1^{(a)}, \dots, \mathbf{y}_{N_a}^{(a)})$ .

Partial correlations between variables can be calculated from these precision matrices, which measure the conditional dependence between variable pairs. Specifically, partial correlation quantifies the correlation between a pair of variables while conditioning on all other variables in the system, thereby isolating direct effects by accounting for potential

<sup>1</sup>When referring to the covariate value, we use ‘ $a$ ’, and when referring to networks or data that corresponds to a covariate value  $a$  we use ‘ $(a)$ ’.

confounding variables, mediators or colliders. Mathematically, the partial correlation between nodes  $i$  and  $j$  in network  $(a)$  is given by

$$\rho_{ij}^{(a)} = -\frac{\Omega_{ij}^{(a)}}{\sqrt{\Omega_{ii}^{(a)} \Omega_{jj}^{(a)}}}, \quad i \neq j,$$

where  $\Omega_{ij}^{(a)}$  is the  $ij$ 'th entry of  $\Omega^{(a)}$ . Thus, if an entry of the precision matrix is non-zero, there is conditional dependence between the corresponding nodes (and vice versa). The edge set  $E^{(a)}$  of the corresponding GGM is then given by  $E^{(a)} = \{(i, j) \mid \Omega_{ij}^{(a)} \neq 0\}$ . Note that because  $\Omega^{(a)}$  is symmetrical,  $(i, j) \in E^{(a)} \Leftrightarrow (j, i) \in E^{(a)}$ .

## 2.2 Graphical spike-and-slab model

To induce sparsity, our proposed approach, NExON-Bayes, relies on a continuous spike-and-slab prior on the off-diagonal elements of each  $\Omega^{(a)}$ , similarly as in Wang et al. (2015) Wang [2015]. This is achieved by using a mixture of two Gaussian distributions, one with very low variance (the spike) and the other with high variance (the slab). A binary edge inclusion indicator is also introduced within this prior, which is denoted as  $\delta_{ij}^{(a)}$ , corresponding to the  $ij$ 'th entry of  $\Omega^{(a)}$ . Edge inclusion is indicated by  $\delta_{ij}^{(a)} = 1$ , while edge exclusion is indicated by  $\delta_{ij}^{(a)} = 0$ . The spike-and-slab prior is thus represented as

$$\Omega_{ij}^{(a)} \mid \delta_{ij}^{(a)} \sim \delta_{ij}^{(a)} \mathcal{N}(0, \nu_1^2) + (1 - \delta_{ij}^{(a)}) \mathcal{N}(0, \nu_0^2), \quad \nu_0^2 \ll \nu_1^2,$$

for  $1 \leq i < j \leq P, i \neq j$ . A symmetric matrix is formed by mirroring this lower triangle across the diagonal.

## 2.3 Dependence on ordinal covariates

NExON-Bayes introduces dependence on an ordinal covariate via a probit submodel placed on the edge inclusion indicator which creates covariate dependence on an edge's probability of inclusion:

$$\delta_{ij}^{(a)} \mid \zeta_{ij}, \beta_{ij} \sim \text{Bernoulli} \{ \Phi(\zeta_{ij} + a\beta_{ij}) \},$$

where  $\Phi(\cdot)$  is the standard normal cumulative distribution function. The parameter  $\beta_{ij}$  is an edge-specific regression coefficient quantifying the influence of the covariate on the inclusion of edge  $(i, j)$ . Specifically,  $\beta_{ij} = 0$  means no relationship between covariate value and edge inclusion probability, i.e., edge  $(i, j)$  has the same probability of being present or absent in *all* networks. A positive value of  $\beta_{ij}$  means that edge inclusion is more likely in networks with high covariate values and vice versa. In addition,  $\zeta_{ij}$  captures the varying baseline inclusion probability of edges and acts as an offset within the probit submodel. We assign a Gaussian prior distribution to  $\beta_{ij}$ ,

$$\beta_{ij} \sim \mathcal{N}(0, \sigma^2),$$

where its hyperparameter  $\sigma^{-2}$  is assigned a Gamma prior,

$$\sigma^{-2} \sim \text{Gamma}(\alpha_\sigma, \beta_\sigma), \quad \alpha_\sigma = \beta_\sigma = 2.$$

Each  $\zeta_{ij}$  is assigned a Gaussian prior,

$$\zeta_{ij} \sim \mathcal{N}(n_0, t_0^2),$$

where the parameters  $n_0$  and  $t_0^2$  are fixed following Xi and Ruffieux [2024] to prior beliefs about the mean and variance of the number of edges in the networks, and thus the overall sparsity.

## 2.4 Variational inference algorithm

Stochastic sampling algorithms like Markov chain Monte Carlo (MCMC) are typically computationally demanding for large graphical models [Wang, 2015]. Instead, we employ deterministic inference algorithms which have been successfully applied in graphical modelling contexts, see, e.g., Li and McCormick [2019], Lingjærde et al. [2024], Xi and Ruffieux [2024]. Specifically, we develop a variational Bayes expectation conditional maximisation (VBECM) algorithm. The true posterior distribution can be written as  $p(\underline{\Omega}, \Theta \mid \mathbf{y})$ , where  $\underline{\Omega} = \{\Omega^{(a)}\}_{a \in \mathcal{A}}$  and  $\Theta$  is the set of all

variables outside of the precision matrix. This true distribution is approximated by using a variational distribution with mean-field approximations:

$$q(\underline{\Omega}, \Theta) = \prod_{a \in \mathcal{A}} q(\Omega^{(a)}) \prod_{a \in \mathcal{A}} \prod_{i < j} q(\delta_{ij}^{(a)}, z_{ij}^{(a)}) \prod_{i < j} q(\zeta_{ij}) q(\sigma^{-2}) \prod_{i < j} q(\beta_{ij}), \quad (2)$$

where  $z_{ij}^{(a)}$  is introduced by reparametrising  $\delta_{ij}^{(a)}$  as:

$$\delta_{ij}^{(a)} | z_{ij}^{(a)} = \mathbb{I}\{z_{ij}^{(a)} > 0\},$$

where  $z_{ij}^{(a)} | \zeta_{ij}, \beta_{ij} \sim \mathcal{N}(\zeta_{ij} + a\beta_{ij}, 1)$ .

The inference problem can then be reframed as finding an approximation to the true distribution, denoted  $q(\underline{\Omega}, \Theta)$ , that is as close as possible to the true posterior distribution by minimising the reverse Kullback–Leibler divergence. This is equivalent to maximising the *evidence lower bound* (ELBO),

$$\mathcal{L}(q) = \mathbb{E}_{q(\underline{\Omega}, \Theta)} \{\log p(\mathbf{Y}, \underline{\Omega}, \Theta)\} - \mathbb{E}_{q(\underline{\Omega}, \Theta)} \{\log q(\underline{\Omega}, \Theta)\},$$

[Bishop and Nasrabadi, 2006]. The optimal distribution for the  $n$ -th factor of  $\Theta$ , denoted  $q_n(\Theta_n)$  is found by iteratively taking the expectation of the logarithm of the joint distribution over all the other factors,

$$\log q_n^*(\Theta_n) = \mathbb{E}_{q(\underline{\Omega}, \Theta \setminus \Theta_n)} \{\log p(\mathbf{Y}, \underline{\Omega}, \Theta)\} + \text{constant},$$

where the constant absorbs all terms not depending on  $\Theta_n$ . However, the variational distribution of each  $\Omega^{(a)}$  is intractable; we therefore update  $\underline{\Omega}$  blockwise using a conditional-maximisation step according to Wang [2015].

Finally, we use the extended Bayesian Information Criteria ( $\text{BIC}_\gamma$ ) to select the spike variance  $\nu_0$ .  $\text{BIC}_\gamma$  extends the Bayesian Information Criteria (BIC) with an additional regularisation penalty parameter  $\gamma \in [0, 1]$ . The  $\text{BIC}_\gamma$  of a network-specific graphical estimation,  $\Omega_{est.}^{(a)}$ , can be found using the following equation:

$$\text{BIC}_\gamma(\Omega_{est.}^{(a)}) = \underbrace{-2\ell(\Omega_{est.}^{(a)}) + |E^{(a)}| \log(N_a)}_{=\text{BIC}} + 4\gamma |E^{(a)}| \log(P),$$

where  $\ell(\cdot)$  is the log likelihood and  $|E^{(a)}|$  is the number of edges present in estimated network  $(a)$  [Foygel and Drton, 2010]. The regularisation parameter  $\gamma$  can be tuned to control the sparsity of the estimates. In this paper, we use the default value of  $\gamma = 0.5$ .

To optimise the values of  $\nu_0$ , we use line searches to find a value of  $\nu_0^{(a)}$  that minimises  $\text{BIC}_\gamma(\Omega_{est.}^{(a)})$  for each network  $(a)$  in the vanilla graphical spike-and-slab model, which gives a strong estimate for expected sparsity.

## 3 Results

### 3.1 Simulated Data

We use simulation studies to assess the performance of NExON-Bayes by analyzing how well it can recover the true precision matrix from which simulated data is generated. For this setting, we consider an ordinal covariate taking values  $a \in \mathcal{A} = \{1, 2, 3, 4\}$ . We correspondingly generate  $|\mathcal{A}| = 4$  precision matrices, each with  $P = 100$  nodes, from which we sample normally distributed data according to Equation (1), where the number of observations for each dataset is  $N = 150$ . To start, network (1) is simulated as scale-free, with 100 edges ( $|E| = P$ ) and thus a sparsity of 0.02. ‘Scale-free’ refers to a graph that has a degree distribution that follows a power law, which leads to few nodes having several connected edges (hubs) and most nodes having very few connected edges. This trait emulates generic biological networks, which are often scale-free [Barabási and Bonabeau, 2003]. The other networks are then created by altering the entries of this first network. Specifically, the zero-valued partial correlations corresponding to 50 edges that are not present in this network (1) are simulated to linearly increase with the value of the covariate  $a$ . Similarly, the non-zero valued partial correlations corresponding to 50 edges that are present in this network (1) are simulated to linearly diminish to zero, such that they are not present in network (4). The remaining 50 edges present in network (1) are present in all four networks, with unchanged partial correlation values. We call edges with increasing partial correlation ‘‘appearing’’ edges and those with decreasing partial correlation ‘‘disappearing’’ edges.

Simulating precision matrices in this way gives rise to an interesting artefact: appearing and disappearing edges have smaller precision matrix entries in networks (2) and (3) and are thus more difficult to uncover. These networks are shown schematically in Figure S1 and Section 2.1 of the Supplementary Material which also provides further details of the data generation algorithm.

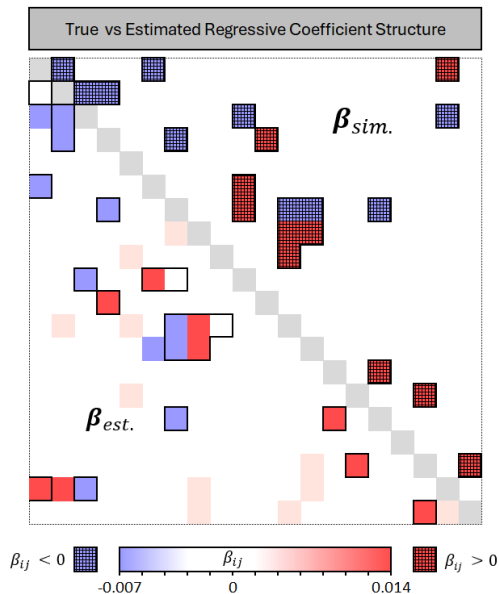


Figure 1: Posterior mean estimates of each  $\beta_{ij}$  (lower diagonal part) versus simulated coefficients of the ordinal covariate (upper diagonal part). Note that there is no real “true”  $\beta$ , as the precision matrices is not simulated from the model. However, there is a known structure based on positive ( $\beta_{ij} > 0$ ) and negative ( $\beta_{ij} < 0$ ) dependencies between covariate and partial correlation. The outline of the true structure is overlain on the estimated structure to ensure a clear comparison (black).

### 3.2 Borrowing information across networks using joint modelling

We now use this simulated data to compare the performance of NExON-Bayes to the standard single-network Bayesian graphical spike-and-slab model (SSL) [Xi and Ruffieux, 2024, Li and McCormick, 2019], upon which our extension is built. Specifically, we evaluate whether introducing a direct relationship between a covariate and the posterior probability of edge inclusion (PPI) indeed boosts statistical power – as a first sanity check that the model behaves as it is meant to.

Table 1 indicates improved area under the curve (AUCs) with NExON-Bayes compared to SSL applied to each network individually. This holds for the estimates of all four networks, with a marked difference in the second and third networks – suggesting that the borrowing of information enabled by the joint modelling is particularly beneficial when NExON-Bayes is used for estimating networks with weaker signals.

Table 1: AUCs for NExON-Bayes and SSL for each simulated network. Standard deviations are in brackets, and the highest AUC for each network is shown in bold.

Network	SSL	NExON-Bayes
1	0.966 (0.004)	<b>0.974</b> (0.003)
2	0.870 (0.007)	<b>0.967</b> (0.003)
3	0.857 (0.009)	<b>0.946</b> (0.006)
4	0.980 (0.003)	<b>0.993</b> (0.001)

As discussed earlier, the level of information sharing is controlled by the edge-specific regression coefficient  $\beta_{ij}$ . Not only is the estimation of  $\beta_{ij}$  useful in increasing statistical power, it also provides insight on sample-level heterogeneity in terms of the effect of the sample-level covariate on the graphical structure. We now consider a smaller simulated setting (with  $P = 20$ ) focused on assessing the ability of NExON-Bayes to recover the values of  $\beta_{ij}$ . The results, shown in Figure 1, indicate that NExON-Bayes successfully captures the changes of edges associated with covariates, information which, as we will illustrate in the cancer data analysis, can enable clinically meaningful interpretation of the estimated network structure. Such insights are not captured intrinsically by state-of-the-art single or joint network modelling approaches.

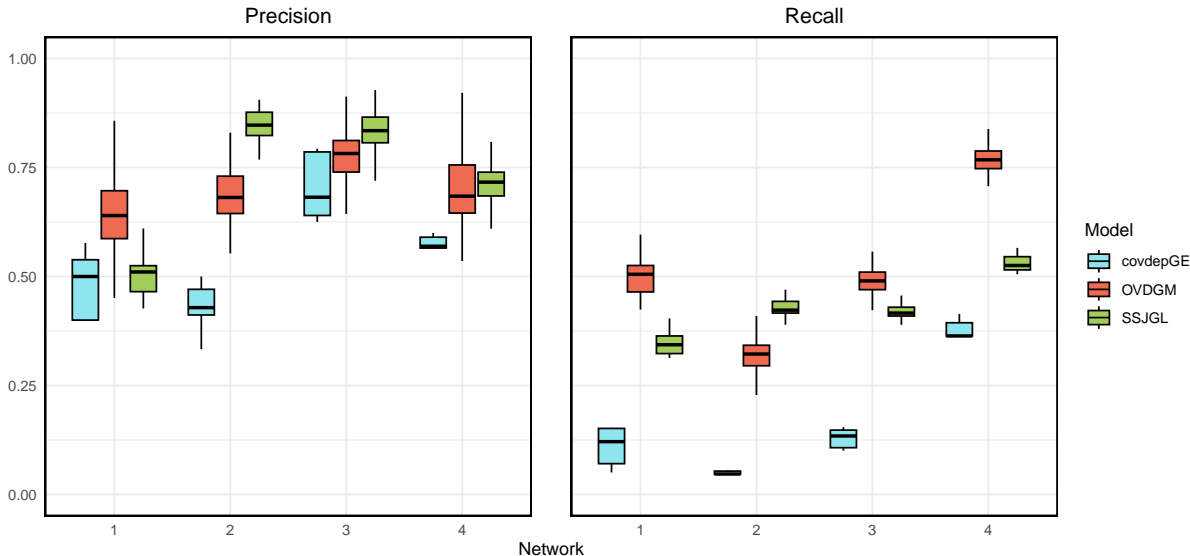


Figure 2: Performance of NExON-Bayes, SSJGL and covdepGE in the simulated scenario where  $P = 100$ ,  $N = 200$  and with 50 edges “appearing” (absolute value of partial correlation linearly increasing with covariate) and 50 edges “disappearing” (absolute value of partial correlation linearly decreasing with covariate). Performance is assessed over 100 replicates for NExON-Bayes and SSJGL and 10 replicates for covdepGE due to excessive runtime (20+ hours).

### 3.3 Comparison to existing joint and covariate-dependent approaches

The performance of NExON-Bayes is then compared against two other models that are representative of the methodology incorporated into our proposal. The first is the *covariate dependent graphical estimation* model (covdepGE) of Helwig et al. (2024) Helwig et al. [2024], which models the precision matrix as a function of the covariate. This approach models the dependence on the covariate via the entries of the precision matrix directly, rather than via the PPI of each edge (as is done in NExON-Bayes). The second approach is the *Bayesian Joint Spike-and-Slab Graphical Lasso* (SSJGL) of Li et al. (2024) Li et al. [2019], which treats the networks as exchangeable, thereby ignoring any inherent ordering among them. Both of these models are extensions of the graphical spike-and-slab model and use a deterministic inference procedure, as in NExON-Bayes.

We assess performance based on *precision*, which measures the proportion of predicted edges that are true positives, and *recall*, which measures the proportion of the true edges that are correctly identified. For NExON-Bayes and covdepGE, we use a 0.5 threshold on the edge PPI to determine edges, based on the median probability model rule [Barbieri and Berger, 2004]. SSJGL does not estimate PPIs and so edges are determined to be present when the corresponding precision matrix entries are non-zero. Figure 2 shows that NExON-Bayes outperforms covdepGE with respect to both precision and recall. The poor performance of covdepGE in this setting can be explained by its overly sparse estimates. By only predicting a low number of edges, the total number of true positive edges will remain low, leading to very poor recall. The precision achieved is also the lowest of any model. Furthermore, covdepGE scales particularly poorly with the number of observations  $N$ , as it models the precision matrix as a continuous function of the covariate, leading to  $|\mathcal{A}| \times N = 600$  precision matrix estimates rather than  $|\mathcal{A}| = 4$  estimates returned by each of the other models.

SSJGL and NExON-Bayes perform much more similarly in comparison, yet SSJGL estimates networks with slightly higher precision but much lower recall in most cases, particularly in networks (1) and (4). This is because SSJGL infers a shared similarity structure across all networks and uses it to inform the network estimates. In this simulated setting, edges that “appear” are mutual to networks (2), (3) and (4), whilst edges that “disappear” are mutual to networks (1), (2) and (3). Therefore, these edges are often estimated as present in all networks even if they are absent in networks (1) and (4) due to the model’s tendency to over-estimate the level of similarity. This is explored further in Section 2.2 of the Supplementary Material. Section 2.3 of the Supplementary Material gives an analysis of computational runtime, which shows that NExON-Bayes achieves the best scalability among the models that estimate multiple networks (see Figure S2 of the Supplementary Material). For up to 6 networks with up to 150 variables ( $P \leq 150$ ), NExON-Bayes runs in less than 20 minutes. SSJGL is up to an order of magnitude slower than this, whilst covdepGE is excessively slow to the point of infeasibility.

Table 2: Results of the gene set enrichment analysis for the two sub-networks with the largest positive  $\beta_{ij}$  estimates and the smallest negative  $\beta_{ij}$  estimates using NExON-Bayes and SSL. Gene sets that are uniquely found by NExON-Bayes but not by SSL and vice versa, are listed in the corresponding columns.

$\beta_{ij} > 0$ (NExON-Bayes)	$\beta_{ij} > 0$ (SSL)	$\beta_{ij} < 0$ (NExON-Bayes)	$\beta_{ij} < 0$ (SSL)
- Apoptosis modulation and signaling - TNF $\alpha$ signaling - Leptin and adiponectin - WNT $\beta$ Catenin signaling - ATM signaling	/	- Acute Viral Myocarditis - TNF $\alpha$ signaling	- Amyotrophic Lateral Sclerosis - Photodynamic therapy induced AP1 survival signaling

### 3.4 Real-World Application

We consider proteomic data from The Cancer Genome Atlas (TCGA) [The Cancer Genome Atlas, 2025], specifically, reverse phase protein array data of patients that have been diagnosed with stage I, II and III breast carcinoma<sup>2</sup> (BRCA). These data have been preprocessed using replicate-based normalisation [Goldman et al., 2020], and contain the expression levels of  $P = 131$  target proteins for  $N_1 = 113$  stage I,  $N_2 = 429$  stage II and  $N_3 = 140$  stage III individuals. We treat tumour stage as our ordinal covariate capturing patient heterogeneity. Although factors like hormonal status also contribute to heterogeneity, we focus on tumour stage as an ordinal covariate to capture broad trends across disease progression. Our aim is to characterize how tumour severity impacts the proteomic network and whether conditional dependencies between protein pairs strengthen or weaken with tumour progression.

NExON-Bayes’s framework provides unique insights into molecular networks by estimating covariate dependencies. In essence, inspecting the edges corresponding to the largest absolute posterior point estimates of  $\beta_{ij}$  could help identify biological processes that characterise tumour progression when used to estimate the proteomic networks of BRCA patients. Figure 3 shows the subnetworks consisting of the edges corresponding to the 50 smallest negative values and the 50 largest positive values of the posterior mean estimate of  $\beta_{ij}$ . To assess whether the borrowing of information facilitated through the inclusion of the edge-specific  $\beta_{ij}$  is beneficial in this setting, we then perform a ranked *gene set enrichment analysis* (GSEA) on the two resulting subnetworks. For each subnetwork, the proteins are ranked by the sum of all adjacent absolute posterior means of  $\beta_{ij}$ . This way, the proteins are ranked according to the overall strength of their covariate dependencies. To perform a GSEA for the networks estimated by SSL, we need to find an equivalent network that expresses the correlations between precision matrix entry and covariate. To do this, we use ordinary least squares regression to find the regressive coefficients between each precision matrix entry and covariate. The proteins are then ranked similarly as before using sum of adjacent regressive coefficients.

Table 2 shows the results of the GSEA, where many more unique gene sets are identified by NExON-Bayes compared to SSL. Of these, several are of interest with relation to BRCA. For instance, the *apoptosis modulation and signaling* pathway refers to programmed cell death, a vital process that maintains tissue homeostasis by eliminating damaged or unnecessary cells. In cancer, the evasion of apoptosis allows malignant cells to survive and proliferate uncontrollably. As such, the pathway controlling apoptotic modulation and signaling plays an important role in the progression of cancer [Plati et al., 2011].

Another gene set of interest in this setting is the *Tumor Necrosis Factor- $\alpha$  signaling* pathway, which is uniquely found in both the “positive” and “negative” networks estimated by NExON-Bayes but in neither estimated by SSL. Tumor necrosis factor- $\alpha$  (TNF $\alpha$ ) is a proinflammatory cytokine that plays a significant role in various cellular processes, including proliferation, differentiation, apoptosis and immune responses. TNF $\alpha$  signaling can therefore either promote or inhibit tumor progression, depending on the cellular environment and specific signaling pathways activated [Agrawal et al., 2023].

Lastly, the *Ataxia Telangiectasia Mutated (ATM) Protein signaling* gene set is found uniquely enriched in the positive network of NExON-Bayes. The ATM signaling pathway plays a key role in breast cancer by maintaining genomic stability and influencing treatment responses. As an important regulator of the DNA damage response, ATM mutations can lead to increased susceptibility to malignancy and impact tumor progression [Varadhan et al., 2024].

The ability to uncover these gene sets through encapsulating sample-level heterogeneity effectively in a joint model is an important practical advantage of NExON-Bayes. We have shown that, by taking this joint approach, interesting

<sup>2</sup>Stage I BRCA refers to tumours that have not spread beyond the breast and are still small in size, stage II refers to slightly larger tumours that may have spread to 1-3 lymph nodes, whilst stage III cancer refers to cancer that has spread to the “lymph nodes, the skin of the breast or the chest muscle” and is larger in size [Macmillan Cancer Support, 2023].

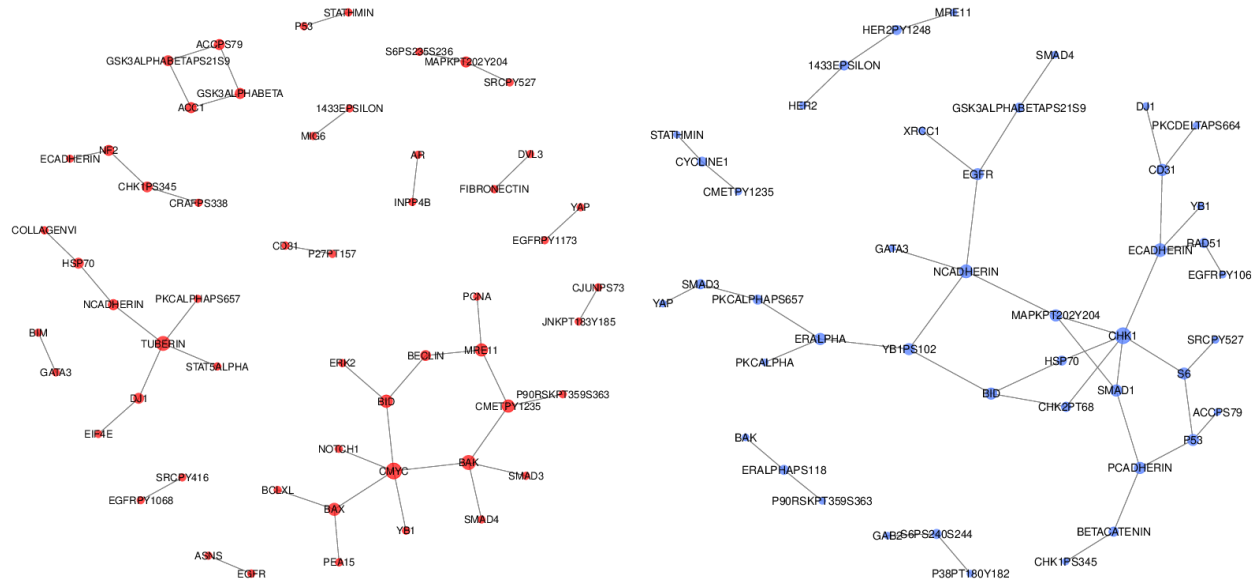


Figure 3: Subnetworks showing the edges with the largest absolute posterior point estimates of  $\beta_{ij}$  in the BRCA application. The left network shows the edges with the largest positive  $\beta_{ij}$  values, and the right network shows the edges with the smallest negative  $\beta_{ij}$  values.

validated or candidate disease mechanisms are uncovered in a disease which progresses through defined stages. These mechanisms warrant dedicated investigation beyond the scope of this paper.

Finally, to further validate the estimations made by NExON-Bayes, we consult the STRING database [Szklarczyk et al., 2023], which contains protein-protein interactions that have been experimentally validated to a given confidence level. We calculate the percentage of pathways that are found by NExON-Bayes and SSL that have been validated to a 90% confidence threshold and show that NExON-Bayes finds a higher percentage of these validated pathways than SSL for all three BRCA stages (see Section 3 of the Supplementary Material).

## 4 Discussion

We have introduced a new method, NExON-Bayes, that jointly estimates multiple graphical models while accounting for sample-level heterogeneity as encapsulated in auxiliary ordinal covariate information. We show that, for such auxiliary data, NExON-Bayes’ formulation better captures sample-level heterogeneity than network estimation models that use continuous covariates (covdepGE) or treat pre-defined groups of samples in an exchangeable manner, without resorting to covariate information (SSJGL). Moreover, thanks to its efficient deterministic inference procedure, our approach is more scalable and better suited to the analysis of current real data settings. Applying our novel methodology to the TCGA breast cancer data set reveals new molecular pathways that characterize tumour stage progression, which could lead to new hypotheses about plausible oncogenic mechanisms.

Several avenues for future work could be considered. First, the current prior formulation assumes a linear relationship between the ordinal variable and the probability of edge inclusion – relaxing this linearity assumption through an alternative monotonic parametric formulation may enhance both the model performance and its biological relevance. Second, as is typical for joint network estimation models, unequal sample sizes can lead to varying levels of sparsity in the estimated networks, reflecting differences in statistical power. This behaviour can in fact be desirable, as smaller sample sizes naturally yield sparser estimates, reducing the risk of false positives. However, if the goal is to isolate true biological variation independent of sample size effects, this pattern can be adjusted for — though doing so will require methodological advances beyond current approaches [Das et al., 2020].

NExON-Bayes offers a principled framework for joint network inference that incorporates sample-level covariates. By uncovering both shared and covariate-dependent patterns of conditional dependence, it enables the systematic characterization of sample-level heterogeneity and supports biologically grounded hypothesis generation for downstream validation.

## Funding and access

This research was supported by the Lopez–Loreta Foundation (J.F., H.R., C.L., X.X.). C.L. has also received funding from the European Union’s Horizon Europe research and innovation programme under the Marie Skłodowska-Curie grant agreement No.101126636. For the purpose of open access, the authors have applied a Creative Commons Attribution (CC BY) license to any Author Accepted Manuscript version arising.

## References

- Ayushi Agrawal, Hasan Balci, Kristina Hanspers, Susan L Coort, Marvin Martens, Denise N Slenter, Friederike Ehrhart, Daniela Digles, Andra Waagmeester, Isabel Wassink, Tooba Abbassi-Daloi, Elisson N Lopes, Aishwarya Iyer, Javier Millán Acosta, Lars G Willighagen, Kozo Nishida, Anders Riutta, Helena Basaric, Chris T Evelo, Egon L Willighagen, Martina Kutmon, and Alexander R Pico. Wikipathways 2024: next generation pathway database. *Nucleic Acids Research*, 52(D1):D679–D689, 11 2023. ISSN 0305-1048. doi: 10.1093/nar/gkad960. URL <https://doi.org/10.1093/nar/gkad960>.
- Albert-László Barabási and Eric Bonabeau. Scale-free networks. *Scientific american*, 288(5):50–9, 2003.
- Maria Maddalena Barbieri and James O Berger. Optimal predictive model selection. *Annals of Statistics*, pages 870–897, 2004.
- Christopher M Bishop and Nasser M Nasrabadi. *Pattern recognition and machine learning*, volume 4. Springer, 2006.
- Liyang Chen, Satwik Acharyya, Chunyu Luo, Yang Ni, and Veerabhadran Baladandayuthapani. Graphr: A probabilistic modeling framework for genomic networks incorporating sample heterogeneity. *Available at SSRN 4849128*, 2024.
- Priyam Das, Christine B Peterson, Kim-Anh Do, Rehan Akbani, and Veerabhadran Baladandayuthapani. Nexus: Bayesian simultaneous network estimation across unequal sample sizes. *Bioinformatics*, 36(3):798–804, 2020.
- Jianqing Fan, Yang Feng, and Yichao Wu. Network exploration via the adaptive lasso and scad penalties. *Annals of Applied Statistics*, 3(2):521–541, 2009.
- Rina Foygel and Mathias Drton. Extended Bayesian information criteria for Gaussian graphical models. *Advances in neural information processing systems*, 23, 2010.
- Jerome Friedman, Trevor Hastie, and Robert Tibshirani. Sparse inverse covariance estimation with the graphical lasso. *Biostatistics*, 9(3):432–441, 2008.
- Mary J Goldman, Brian Craft, Mim Hastie, Kristupas Repečka, Fran McDade, Akhil Kamath, Ayan Banerjee, Yunhai Luo, Dave Rogers, Angela N Brooks, Jingchun Zhu, and David Haussler. Visualizing and interpreting cancer genomics data via the xena platform. *Nature Biotechnology*, 38:675–678, 2020. doi: 10.1038/s41587-020-0546-8.
- Jian Guo, Elizaveta Levina, George Michailidis, and Ji Zhu. Joint estimation of multiple graphical models. *Biometrika*, 98(1):1–15, 2011.
- Jacob Helwig, Sutanoy Dasgupta, Peng Zhao, Bani K Mallick, and Debdeep Pati. Algorithm 1045: A covariate-dependent approach to Gaussian graphical modeling in r. *ACM Transactions on Mathematical Software*, 2024.
- Zehang Li, Tyler McCormick, and Samuel Clark. Bayesian joint spike-and-slab graphical Lasso. In Kamalika Chaudhuri and Ruslan Salakhutdinov, editors, *Proceedings of the 36th International Conference on Machine Learning*, volume 97 of *Proceedings of Machine Learning Research*, pages 3877–3885. PMLR, June 2019. URL <https://proceedings.mlr.press/v97/li19h.html>.
- Zehang Richard Li and Tyler H McCormick. An expectation conditional maximization approach for gaussian graphical models. *Journal of Computational and Graphical Statistics*, 28(4):767–777, 2019.
- Camilla Lingjærde and Sylvia Richardson. Stabjgl: a stability approach to sparsity and similarity selection in multiple-network reconstruction. *Bioinformatics Advances*, 3(1):vbad185, 2023.
- Camilla Lingjærde, Benjamin P Fairfax, Sylvia Richardson, and Hélène Ruffieux. Scalable multiple network inference with the joint graphical horseshoe. *The Annals of Applied Statistics*, 18(3):1899–1923, 2024.
- Jing Ma and George Michailidis. Joint structural estimation of multiple graphical models. *Journal of Machine Learning Research*, 17(166):1–48, 2016.
- Macmillan Cancer Support. Stages and grades of breast cancer, 2023. URL <https://www.macmillan.org.uk/cancer-information-and-support/breast-cancer/staging-and-grading-of-breast-cancer>. [Accessed: 26-February-2025].
- Nicolai Meinshausen and Peter Bühlmann. High-dimensional graphs and variable selection with the Lasso. *The Annals of Statistics*, 34(3):1436 – 1462, 2006.

- Jessica Plati, Octavian Bucur, and Roya Khosravi-Far. Apoptotic cell signaling in cancer progression and therapy. *Integrative biology*, 3(4):279–296, 2011.
- Damian Szklarczyk, Rebecca Kirsch, Mikaela Koutrouli, Katerina Nastou, Farrokh Mehryary, Radja Hachilif, Annika L Gable, Tao Fang, Nadezhda T Doncheva, Sampo Pyysalo, et al. The string database in 2023: protein–protein association networks and functional enrichment analyses for any sequenced genome of interest. *Nucleic acids research*, 51(D1):D638–D646, 2023.
- The Cancer Genome Atlas. The Cancer Genome Atlas Program, 2025. URL <https://www.cancer.gov/tcga>. Accessed: 2025-03-21.
- Varsha Varadhan, Monica Shri Manikandan, Akshaya Nagarajan, Thirunavukkarasu Palaniyandi, Maddaly Ravi, Senthil Kumar Sankareswaran, Gomathy Baskar, Mugip Rahaman Abdul Wahab, and Hemapreethi Surendran. Ataxia-telangiectasia mutated (atm) gene signaling pathways in human cancers and their therapeutic implications. *Pathology - Research and Practice*, 260:155447, 2024. ISSN 0344-0338. doi: <https://doi.org/10.1016/j.prp.2024.155447>. URL <https://www.sciencedirect.com/science/article/pii/S0344033824003583>.
- Hao Wang. Bayesian graphical Lasso models and efficient posterior computation. *Bayesian Analysis*, 7(4):867–886, 2012.
- Hao Wang. Scaling it up: Stochastic search structure learning in graphical models. *Bayesian Analysis*, 10(2):351–377, 2015.
- Xiaoyue Xi and H el ene Ruffieux. A modeling framework for detecting and leveraging node-level information in Bayesian network inference. *Biostatistics*, 26(1):kxae021, 06 2024. ISSN 1465-4644. doi: 10.1093/biostatistics/kxae021. URL <https://doi.org/10.1093/biostatistics/kxae021>.